(89) J. G. Bergman, Jr., and F. A. Cotton, *Inorg. Chem.*, **5**, 1208 (1966).
(90) C. Bellito, L. Gastaldi, and A. A. G. Tomlinson, *J. Chem. Soc., Dalton Trans.*, 989 (1976).
(91) The related Sn^{IV} (ref 92) species seems to be closer to the Ti^{IV} (d^0) (ref 93) rather than the Zn (d^{10}) system. We shall regard it then as having a d^0 configuration.
(92) C. D. Garner, D. Sutton, and S. C. Wallwork, *J. Chem. Soc. A*, 1949 (1967).
(93) C. C. Addison, C. D. Garner, W. B. Simpson, D. Sutton, and S. C. Wallwork, *Proc. Chem. Soc., London*, 367 (1964).
(94) D. A. Langs and C. R. Hare, *Chem. Commun.*, 890 (1967).
(95) E. L. Muetterties, *Inorg. Chem.*, **4**, 769 (1965).
(96) E. L. Muetterties, *Acc. Chem. Res.*, **3**, 266 (1970).
(97) L. Malatesta, M. Freni, and V. Valenti, *Gazz. Chim. Ital.*, **94**, 1278 (1964).
(98) (a) R. C. Fay, D. F. Lewis, and J. R. Weir, *J. Am. Chem. Soc.*, **97**, 7179 (1975); (b) R. D. Archer and C. J. Donahue, *ibid.*, **99**, 269, 6613 (1977).
(99) R. C. Fay and J. K. Howie, *J. Am. Chem. Soc.*, **99**, 8110 (1977).
(100) J. P. Jesson, E. L. Muetterties, and P. Meakin, *J. Am. Chem. Soc.*, **93**, 5261 (1971).
(101) R. Hoffmann, *J. Chem. Phys.*, **39**, 1397 (1963); R. Hoffmann and W. N. Lipscomb, *ibid.*, **36**, 2179, 3489 (1962); **37**, 2872 (1962).
(102) H. Basch and H. B. Gray, *Theor. Chim. Acta*, **3**, 458 (1965).

Contribution from Le Laboratoire de Chimie des Organométalliques, ERA 477, Université de Rennes, 35031 Rennes Cedex, France, and The Guelph-Waterloo Centre for Graduate Work in Chemistry, Waterloo Campus, Department of Chemistry, University of Waterloo, Waterloo, Ontario N2L 3G1, Canada

Carbon Disulfide Complexes of Zerovalent Iron: Synthesis and Spectroscopic Properties. X-ray Crystal Structure of (η^2-Carbon disulfide)dicarbonyl(trimethylphosphine)(triphenylphosphine)iron(0)

HUBERT LE BOZEC,[1a] PIERRE H. DIXNEUF,*[1a] ARTHUR J. CARTY,*[1b] and NICHOLAS J. TAYLOR[1b]

Received August 18, 1977

Carbon disulfide complexes of iron(0), $Fe(\eta^2\text{-}CS_2)(CO)_2L_2$ [L = $P(OMe)_3$, $P(OEt)_3$, $P(OPh)_3$, PPh_3], have been synthesized from (benzylideneacetone)tricarbonyliron(0) via reaction with tertiary phosphorus ligands in carbon disulfide. An excellent route to the trialkyl- or dialkylarylphosphine complexes $Fe(\eta^2\text{-}CS_2)(CO)_2L_2$ (L = PMe_3, PMe_2Ph, $P(n\text{-}Bu)_3$) or $Fe(\eta^2\text{-}CS_2)(CO)_2(PPh_3)L$ (L = PMe_3, PMe_2Ph) consists of displacing one or two molecules of triphenylphosphine from $Fe(\eta^2\text{-}CS_2)(CO)_2(PPh_3)_2$ by the more nucleophilic phosphines. The mixed phosphine–phosphite derivative $Fe(\eta^2\text{-}CS_2)(CO)_2(PMe_3)(P(OMe)_3)$ can be obtained from $Fe(\eta^2\text{-}CS_2)(CO)_2(PMe_3)(PPh_3)$ via PPh_3 substitution. These compounds have been characterized by microanalyses, by IR, ^1H and ^{31}P NMR and mass spectroscopy, and for $Fe(\eta^2\text{-}CS_2)(CO)_2(PMe_3)(PPh_3)$ by single-crystal X-ray diffraction. Crystals of $Fe(\eta^2\text{-}CS_2)(CO)_2(PMe_3)(PPh_3)$ are monoclinic, space group *Pc*, with $a = 9.309$ (4) Å, $b = 13.640$ (12) Å, $c = 11.390$ (5) Å, $\beta = 120.43$ (5)°, and $Z = 2$. The structure was solved by Patterson and Fourier techniques using 1881 independent, counter-measured reflections for which $I \geq 3\sigma(I)$. Refinement by full-matrix least-squares methods with all nonhydrogen atoms having anisotropic thermal parameters converged at $R = 0.039$ and $R_w = 0.046$. The CS_2 ligand is η^2 coordinated and the iron stereochemistry is best described as trigonal bipyramidal with trans phosphorus ligands and the coordinated C=S bond of the CS_2 molecule occupying an equatorial position. Important bond lengths are C(3)–S(1) = 1.676 (7), C(3)–S(2) = 1.615 (8), Fe–S(1) = 2.334 (2), Fe–C(3) = 1.983 (8), Fe–P(1) = 2.279 (2), and Fe–P(2) = 2.252 (2) Å. The electronic nature of the bound CS_2 ligand is discussed in the light of structural and spectroscopic parameters.

Introduction

Transition-metal η^2-CS_2 complexes are the main precursors to thiocarbonyl compounds.[2a] The transformation of an η^2-CS_2 molecule to a thiocarbonyl is achieved either by removal of one sulfur atom as phosphine sulfide on treatment with a tertiary phosphine or via alkylation of the uncoordinated sulfur atom followed by alkylthiol elimination on subsequent reaction with acid[2a] or hydride ion[2b] (Scheme I). Moreover, η^2-CS_2 complexes are highly activated toward electrophilic reagents. The uncoordinated sulfur atom behaves as a strong nucleophile, displacing halide ion from alkyl halides to give sulfur alkylated cations[3] or weakly bound ligands from other organometallic derivatives leading to CS_2-bridged binuclear complexes.[4,5] Another interesting feature of CS_2 coordination chemistry concerns the electron-donor–electron-acceptor properties of this ligand. Recent spectroscopic evidence[6] may point to an acceptor capability for η^2-CS_2 in η^5-$C_5H_5Mn(CO)_2L$ complexes superior to that of CO and comparable with that of CS or PF_3.

Despite their synthetic utility and potential, relatively few η^2-CS_2 complexes of first-row transition metals have been characterized.[2a] We report herein the synthesis of a series of η^2-CS_2 complexes of the type $Fe(\eta^2\text{-}CS_2)(CO)_2LL'$ (L, L' = tertiary phosphine or phosphite) for which a versatile chemistry can be anticipated. The spectroscopic characterization of these complexes is described. An X-ray crystal structure analysis of $Fe(\eta^2\text{-}CS_2)(CO)_2(PMe_3)(PPh_3)$ has been carried out to provide the first accurate structural parameters for a first-row transition-metal CS_2 derivative and to form a basis for spectroscopic investigations of CS_2–M bonding.

Scheme I

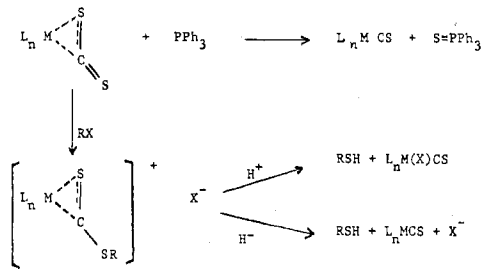

Experimental Section

General Methods. Infrared spectral determinations were made using a Beckman IR 12 spectrophotometer. Frequencies are accurate to ±2 cm^{-1}. NMR spectra were recorded on a Varian EM 360 (^1H; $CDCl_3$ solution with Me_4Si internal standard unless otherwise noted) and a Bruker WH 90 (^{31}P; $CDCl_3$ solution unless otherwise noted; shifts are downfield (+) from external H_3PO_4). Mass spectra were determined at 70 eV using a Varian MAT 311 double-focusing spectrometer. Microanalyses were determined by CNRS microanalyses (THIAIS).

Synthesis. $Fe(\eta^2\text{-}CS_2)(CO)_2[P(OR)_3]_2$ (2a (R = Me), 2b (R = Et), 2c (R = Ph)). The phosphite (2 mmol) was added to a solution of (benzylideneacetone)tricarbonyliron (**1**)[7] (1 mmol) in CS_2 (5 mL)

0020-1669/78/1317-2568$01.00/0

in a Schlenk tube under an argon atmosphere. The mixture was stirred overnight at room temperature. Solvent was eliminated in vacuo and the crude products were chromatographed on thick layer silica gel plates (eluent: hexane–ether). Pure products crystallized from hexane–ether solutions.

2a: yield 35% (0.55 g from 1.1 g of **1** and 1 mL of $P(OMe)_3$); mp 68 °C; IR (cm^{-1}) ν(CO) (THF) 2020, 1964, ν(C=S) (Nujol) 1170; ^1H NMR δ 3.83 (t) ($^3J_{P-H}$ = 11.6 Hz); mass spectrum m/e $|M|^+$ calcd 435.927, found 435.929. Anal. Calcd: C, 24.78; H, 4.16; P, 14.20; S, 14.70. Found: C, 24.90; H, 4.16; P, 14.08; S, 14.41.

2b: yield 20% (0.57 g from 1.6 g of **1** and 2.7 mL of $P(OEt)_3$); mp 63 °C; IR (cm^{-1}) ν(CO) (THF) 2017, 1961, ν(C=S) (Nujol) 1160; ^1H NMR δ 1.32 (t) (CH_3), 4.25 (m) (OCH_2). Anal. Calcd: C, 34.60; H, 5.77. Found: C, 34.21; H, 5.73.

2c: yield 25% (0.50 g from 0.76 g of **1** and 1.4 mL of $P(OPh)_3$); mp 95–100 °C dec; IR (cm^{-1}) ν(CO) (THF) 2027, 1979, ν(C=S) (Nujol) 1160; ^1H NMR δ 7.50 (m). Anal. Calcd: C, 57.92; H, 3.71. Found: C, 57.90; H, 3.85.

Fe(η^2-CS_2)$(CO)_2(PPh_3)_2$ (2d). Complex **1** (1.0 g) and PPh_3 (2.1 g, 8 mmol) were dissolved in CS_2 (20 mL). The solution was stirred overnight at room temperature. After removal of CS_2 in vacuo, the precipitate was washed with ether and ethanol. A 90% yield (2.25 g) of **2d** was obtained; mp 149 °C dec. Agreement was found with reported infrared data.[8] IR (cm^{-1}): ν(CO) (THF) 1999, 1937, ν(C=S) (Nujol) 1155. ^1H NMR (CD_2Cl_2): δ 7.40 (m). ^{31}P NMR (CD_2Cl_2): δ 56.56 (s). Anal. Calcd: C, 65.64; H, 4.21; P, 8.70; S, 8.98; Fe, 7.86. Found: C, 65.38; H, 4.54; P, 8.69; S, 8.53; Fe, 7.85.

Fe(η^2-CS_2)$(CO)_2(PR_3)_2$ (2a (R = OMe), 2e (R = Me), 2f (R_3 = Me_2Ph), 2g (R = Bu)). The phosphorus ligand (2 mmol) was added to a solution of complex **2d** (1 mmol) in dichloromethane (15 mL) in a Schlenk tube. The solution was stirred at reflux temperature for 15 min. The reaction mixture was chromatographed on a silica gel column (eluent: hexane and then hexane–ether) and crystallized from hexane–ether mixtures.

2a: yield 95% (0.87 g from 1.5 g of **2d** and 0.7 mL of $P(OMe)_3$); mp 68 °C.

2e: yield 88% (0.85 g from 2 g of **2d** and 0.6 mL of PMe_3); mp 110 °C; IR (cm^{-1}) ν(CO) (THF) 1991, 1929, ν(C=S) (Nujol) 1135; ^1H NMR δ 1.35 (t) ($^2J_{P-H}$ = 8.8 Hz), ^{31}P NMR δ 17.76 (s); mass spectrum m/e $|M|^+$ calcd 339.9572, found 339.9570. Anal. Calcd: C, 31.76; H, 5.29. Found: C, 31.77; H, 5.12.

2f: yield 85% (1.10 g from 2 g of **2d** and 0.80 mL of PMe_2Ph); mp 70 °C; IR (cm^{-1}) ν(CO) (THF) 1999, 1933, ν(C=S) (Nujol) 1150; ^1H NMR δ 1.65 (t), 1.67 (t) (CH_3) ($^2J_{P-H}$ = 8.6 Hz); mass spectrum m/e $|M - S|^+$ calcd 432.0165, found 432.0158. Anal. Calcd: C, 49.24; H, 4.75. Found: C, 49.13; H, 4.67.

2g: yield 90% (0.75 g from 1 g of **2d** and 0.7 mL of PBu_3); mp 71 °C; IR (cm^{-1}) ν(CO) (THF) 1992, 1927, ν(C=S) (Nujol) 1145; ^1H NMR δ 0.93 (m) (CH_3), 1.49 (m) [$(CH_2)_n$]; ^{31}P NMR (C_6D_6) δ 35.68 (s); mass spectrum m/e $|M - CS_2|^+$ calcd 516.2948, found 516.2954. Anal. Calcd: C, 54.60; H, 9.10; P, 10.45; S, 10.82. Found: C, 54.93; H, 8.97; P, 10.36; S, 10.53.

Fe(η^2-CS_2)$(CO)_2(PPh_3)(PMe_3)$ (3). PMe_3 (0.3 mL) was added to a solution of complex **2d** (2 g) in dichloromethane (20 mL), and the solution was stirred at room temperature for 2.5 h. After removal of solvent the crude solid was washed with pentane (20 mL) and ether (20 mL) and then crystallized from dichloromethane–hexane solutions. A 75% yield (1.10 g) of **3** was isolated: mp 140–145 °C dec; IR (cm^{-1}) ν(CO) (THF) 1994, 1933, ν(C=S) (Nujol) 1160; ^1H NMR δ 1.50 (dd) (CH_3) ($^2J_{P-H}$ = 10 Hz, $^4J_{P-H}$ = 1.1 Hz), 8.0 (m) (C_6H_5); ^{31}P NMR δ 21.67, 54.87 (AB quartet) ($^2J_{P-P}^{trans}$ = 161 Hz). Anal. Calcd: C, 54.76; H, 4.60. Found: C, 54.65; H, 4.52.

Fe(η^2-CS_2)$(CO)_2(PPh_3)(PMe_2Ph)$ (4). PMe_2Ph (0.4 mL) was added to a solution of complex **2d** (2 g) in dichloromethane (20 mL), and the solution was stirred at room temperature for 5 h. Thick layer silica gel chromatography (eluent: ether–hexane) of the crude product followed by crystallization from 1:1 hexane–dichloromethane afforded a 55% yield (0.92 g) of **4:** mp 129 °C; IR (cm^{-1}) ν(CO) (THF) 1999, 1937, ν(C=S) (Nujol) 1150; ^1H NMR δ 1.80 (d) (CH_3) ($^2J_{P-H}$ = 9.5 Hz), 7.70 (m) (C_6H_5). Anal. Calcd: C, 59.10; H, 4.42. Found: C, 58.63; H, 4.39.

Fe(η^2-CS_2)$(CO)_2[P(OMe)_3](PMe_2Ph)$ (5). A solution of **3** (2 g) and $P(OMe)_3$ (0.5 mL) in CH_2Cl_2 (20 mL) was stirred at reflux temperture for 1 h. Thick layer silica gel chromatography (eluant: hexane–ether) of the crude product followed by crystallization from hexane afforded a 71% yield (1.05 g) of **5:** mp 101 °C; IR (cm^{-1}) ν(CO) (THF) 2010, 1943, ν(C=S) (Nujol) 1140; ^1H NMR δ 1.37 (dd) (P–CH_3) ($^2J_{P-H}$ = 10 Hz, $^4J_{P-H}$ = 2 Hz), 3.73 (d) ($POCH_3$) ($^3J_{P-H}$ = 11 Hz); ^{31}P NMR δ 17.69, 166.78 (AX quartet) ($^2J_{P-P}^{trans}$ = 245 Hz). Anal. Calcd: C, 27.84; H, 4.67. Found: C, 27.92; H, 4.61.

Fe(η^2-CS_2)$(CO)[P(OMe)_3](PMe_2Ph)_2$ (6). A solution of **2a** (1.5 g) and PMe_2Ph (15 mL) in CH_2Cl_2 was heated under reflux for 4 h. Chromatography of crude products on thick layer silica gel plates (eluant: 1:1 hexane–ether) afforded as a major fraction complex **6** (0.25 g, 15%) recrystallized from hexane: mp 122 °C; IR (cm^{-1}) ν(CO) (THF) 1904, ν(C=S) (Nujol) 1140; ^1H NMR δ 1.53 (t), 1.67 (t) (P–CH_3) ($^2J_{P-H}$ = 8 Hz), 3.3 (d) ($POCH_3$) ($^3J_{P-H}$ = 11 Hz); ^{31}P NMR δ 22.75 (d) (PMe_2Ph), 178.93 (t) ($P(OMe)_3$) ($^2J_{P-P}^{cis}$ = 55.7 Hz). Anal. Calcd: C, 45.00; H, 5.54. Found: C, 44.40; H, 5.34. No attempt was made to separate other products from this reaction.

X-ray Analysis

Collection and Reduction of the X-ray Data. Yellow-orange prisms of $Fe(CS_2)(CO)_2(PMe_3)(PPh_3)$ were grown from dichloromethane–hexane. Preliminary Weissenberg and precession photographs established that the molecule crystallizes in the monoclinic space group Pc with systematic absences $h0l$; $l \neq 2n$.[9]

This is a nonstandard setting of Pn which can be converted to Pn by the transformation $a' = a$, $b' = b$, and $c' = a + c$, where a, b, and c are the axes of Pc and a', b', and c' are the axes of Pn.

Unit cell dimensions a = 9.309 (4) Å, b = 13.640 (12) Å, c = 11.390 (5) Å, and β = 120.43 (5)° were obtained by least-squares refinement of 2θ values for 29 reflections measured on a Datex automated GE-XRD-6 diffractometer using Mo Kα (λ 0.710 69 Å) radiation. The calculated density of 1.402 g cm^{-3} for Z = 2 and V = 1247 $Å^3$ agrees with the density of 1.39 g cm^{-3} measured by flotation in carbon tetrachloride–hexane and with $F(000)$ = 544.

Intensity data were collected on a well-formed prism of dimensions 0.4 × 0.4 × 0.4 mm mounted with the a^* axis parallel to the ϕ axis of the diffractometer. The θ–2θ scan technique was used and a unique quadrant of data was collected at 297 ± 2 K out to 2θ = 50°. Zirconium-filtered Mo Kα radiation was employed. The integrated intensities were measured with a scintillation counter employing a pulse height analyzer. The diffracted X-ray beam passed through a collimator of 1-mm diameter placed $\simeq$5 cm from the crystal and then to the counter via an aperture approximately 18 cm from the crystal. The takeoff angle was 4°. The scan width was determined by the equation $\Delta\theta = \pm(0.9 + 0.43 \tan\theta)$ and a constant scan rate of 2°/min was used. Stationary-crystal, stationary-counter background counts of 10 s were taken before and after each scan. The intensities of three standard reflections, monitored after every 100 measurements, fell by <5% during the course of data collection. Data were scaled accordingly. From a total of 2202 independent intensity measurements, 1881 with intensities $I \geq 3\sigma(I)$ were counted as observed and used in the solution and refinement. Lorentz and polarization corrections were applied to the determination of structure amplitudes. For these atoms, μ = 9.28 cm^{-1} and no absorption correction was deemed necessary. An error of less than 2% based on $|F|$ would result from failure to correct for absorption.

Structure Solution and Refinement. An unsharpened Patterson synthesis was solved to yield the coordinates of the heavy-metal atom. An initial Fourier synthesis phased with the iron atom revealed the positions of the phosphorus and sulfur atoms together with the carbonyl groups. A subsequent Fourier synthesis was utilized to find the remaining nonhydrogen atoms. With all nonhydrogen atoms having isotropic temperature coefficients the structure was refined by full-matrix least-squares methods to an R value ($R = \sum\|F_o| - |F_c\|/\sum|F_o|$) of 0.073. Heavy-atom scattering functions were taken from ref 10 with corrections included for both the real and imaginary parts of the anomalous dispersion for iron. Hydrogen values were those of Stewart et al.[11] Conversion to anisotropic temperature coefficients followed by two further cycles of refinement gave R = 0.046. A difference Fourier synthesis calculated at this stage revealed locations for all of the hydrogen atoms. These were included in the refinement (334 parameters) but methyl group hydrogen atom positional parameters were fixed. A weighting scheme of the type $w^{-1} = 10.0 - 0.3|F| + 0.015|F|^2$ was then introduced to give constant errors in the various ranges of $|F_o|$. The refinement converged at R = 0.036 with the weighted residual R_w ($R_w = [\sum_w(|F_o| - |F_c|)^2/\sum_w F_o^2]^{1/2}$) of 0.043. A final difference Fourier synthesis revealed

Table I. Atomic Coordinates (Fractional × 10^4) for $Fe(\eta^2\text{-}CS_2)(CO)_2(PMe_3)(PPh_3)$

	x	y	z
Fe	0000	2429.6 (5)	5000
S(1)	1516 (2)	3876 (1)	5395 (2)
S(2)	4115 (2)	2260 (2)	6001 (2)
P(1)	−892 (2)	2577.9 (9)	2739 (1)
P(2)	747 (2)	2323 (1)	7211 (2)
O(1)	602 (8)	341 (3)	4994 (6)
O(2)	−3329 (6)	2731 (5)	4574 (5)
C(1)	369 (8)	1129 (4)	4973 (6)
C(2)	−2037 (7)	2623 (4)	4707 (5)
C(3)	2342 (8)	2756 (4)	5577 (6)
C(4)	618 (16)	3473 (7)	7945 (9)
C(5)	2778 (13)	1823 (12)	8371 (9)
C(6)	−590 (17)	1537 (11)	7527 (10)
C(11)	757 (7)	2683 (4)	2331 (5)
C(12)	1660 (8)	1854 (5)	2388 (7)
C(13)	2920 (9)	1910 (5)	2102 (7)
C(14)	3360 (7)	2805 (6)	1800 (6)
C(15)	2523 (9)	3633 (5)	1799 (7)
C(16)	1215 (8)	3575 (4)	2031 (6)
C(21)	−2152 (7)	1554 (4)	1678 (5)
C(22)	−2130 (9)	1254 (5)	506 (6)
C(23)	−3142 (10)	489 (6)	−282 (8)
C(24)	−4172 (9)	21 (5)	48 (7)
C(25)	−4247 (8)	311 (5)	1188 (7)
C(26)	−3215 (7)	1072 (4)	1991 (6)
C(31)	−2277 (7)	3620 (4)	1868 (6)
C(32)	−2457 (9)	4390 (5)	2576 (7)
C(33)	−3553 (11)	5171 (6)	1868 (9)
C(34)	−4480 (10)	5180 (6)	486 (8)
C(35)	−4321 (11)	4412 (7)	−237 (8)
C(36)	−3221 (10)	3641 (6)	438 (8)

Scheme II

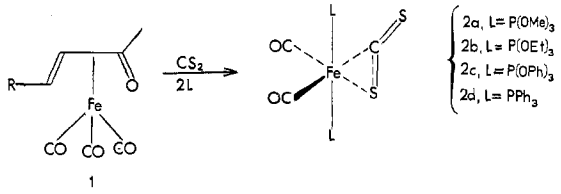

1

a general background of ≃0.5 e Å^{-3} with no peaks higher than 1.2 e Å^{-3}. The observed and calculated structure factor amplitudes are available as supplementary data.

Final positional parameters for nonhydrogen atoms are listed in Table I with anisotropic thermal parameters in Table II. Supplementary Table S1 contains hydrogen atom positions and isotropic thermal parameters. Important bond lengths and angles are gathered in Table III with carbon–hydrogen distances in supplementary Table S2. Table IV contains a selection of relevant least-squares planes.

Results and Discussion

Synthesis. Heterodiene iron tricarbonyls such as the benzylideneacetone complex **1** (R = Ph)[7] *readily* add nucleophilic phosphines and phosphites.[12] Stable adducts are formed by displacement of the ketonic carbonyl group only. The easily accessible complex **1** also reacts with carbon disulfide, but in this case no stable adduct could be isolated. Addition of tertiary phosphites to this carbon disulfide solution effected complete removal of the heterodiene giving the η^2-CS_2 complexes **2a–c** (Scheme II). These compounds were purified by column or thick-layer chromatography followed by recrystallization from dichloromethane–hexane or ether–hexane mixtures under argon or nitrogen. The crystalline complexes (and other compounds synthesized herein) are quite air stable in the solid state and can even be handled in solution in air for limited periods. The trans stereochemistry of **2a** was evident from its ^{1}H NMR parameters (vide infra).

This method of formation of η^2-CS_2–Fe complexes is effective only for phosphorus ligands which are inert toward CS_2, such as phosphites or arylphosphines. Triphenylphosphine gave

Scheme III

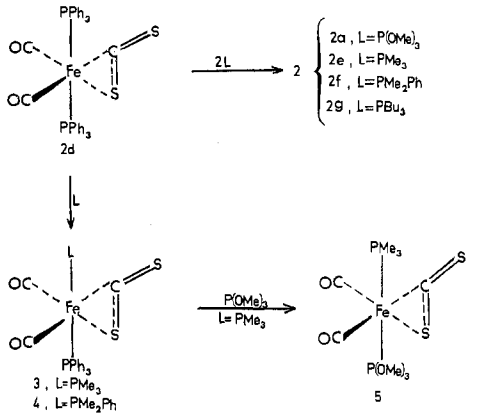

Scheme IV

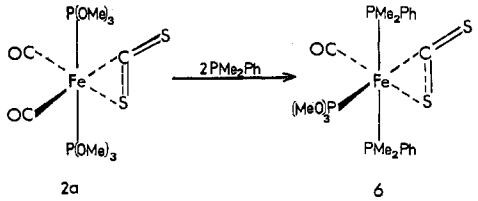

complex **2d** in 90% yield. This derivative had been prepared previously by Baird, Hartwell, and Wilkinson[8] starting from $Fe_2(CO)_9$.

Alkylphosphines which form zwitterionic adducts with CS_2 gave only low yields (<5%) of complexes **2** starting with CS_2 solutions of (α-enone)$Fe(CO)_3$. However, an excellent alternative route to the trialkyl- or dialkylarylphosphine complexes **2e–g** is via displacement of triphenylphosphine from derivative **2d**. The bis(trimethyl phosphite) complex **2a** was also obtained in good yield by this substitution route which occurs with retention of the trans configuration of the bis(phosphine) complexes (Scheme III).

The selective replacement of one triphenylphosphine ligand from **2d** was accomplished by using 1:1 molar ratios of **2d** and the nucleophilic phosphines PMe_3 or PMe_2Ph. Thus the unsymmetrical derivatives **3** and **4** were synthesized in good yields.

The availability of derivatives containing trialkylphosphines and phosphites is significant since these compounds are considerably more soluble in nonpolar solvents and are more volatile than **2b**. In addition the alkylphosphine complexes have greater thermal stability than **2d**. These characteristics lend themselves to synthetic application.

It is of interest that the substitution of triphenylphosphine in **2d** by $P(OMe)_3$, PMe_3, PMe_2Ph, and PBu_3 proceeds in virtually quantitative fashion. This result is, at least in part, predictable since PPh_3 has a greater cone angle than the incoming ligands. Tolman's studies on nickel(0)–phosphine equilibria have clearly demonstrated the importance of steric bulk in phosphine substitution reactons.[13] Although no detailed equilibria studies have been carried out for the reaction $Fe(CS_2)(CO)_2(PPh_3)_2 + 2L \rightleftharpoons Fe(CS_2)(CO)_2L_2 + 2PPh_3$, it is clear from the preparative work that this equilibrium lies far to the right. This is also apparent for monosubstitution on **2d** by PMe_3 and PMe_2Ph. Moreover, reacting compound **3** with 1 equiv of $P(OMe)_3$ afforded 71% of derivative **5**. The substitution route **2d** → **3** → **5** indicates a facile method for selectively introducing unsymmetrical ligands into the apical position. The transformation **3** → **5** clearly shows the greater lability of the Fe–PPh_3 bond as compared to the Fe–PMe_3 bond toward poorer nucleophiles, smaller than triphenylphosphine. By contrast, the reaction of **2a** containing the small

Table II. Anisotropic[a] Thermal Parameters ($\times 10^4$) for $Fe(\eta^2\text{-}CS_2)(CO)_2(PMe_3)(PPh_3)$

	β_{11}	β_{22}	β_{33}	β_{12}	β_{13}	β_{23}
Fe	121 (1)	39.9 (4)	66.6 (7)	0.4 (6)	39.0 (7)	−2.8 (5)
S(1)	207 (3)	45.4 (9)	136 (2)	−13 (1)	76 (2)	−13 (1)
S(2)	129 (3)	84 (1)	187 (3)	8 (2)	68 (2)	−0 (2)
P(1)	118 (2)	34.5 (8)	66 (2)	4 (1)	46 (2)	2.7 (9)
P(2)	160 (3)	66 (1)	63 (2)	8 (1)	35 (2)	0 (1)
O(1)	338 (14)	50 (3)	165 (8)	28 (5)	95 (8)	11 (4)
O(2)	124 (8)	148 (6)	127 (7)	10 (5)	63 (6)	−18 (5)
C(1)	198 (14)	54 (4)	71 (6)	−23 (6)	28 (7)	12 (4)
C(2)	146 (12)	65 (4)	51 (6)	−14 (5)	35 (6)	−16 (4)
C(3)	169 (12)	51 (3)	89 (7)	−28 (5)	48 (8)	−21 (4)
C(4)	510 (35)	98 (7)	136 (12)	55 (13)	161 (18)	−22 (7)
C(5)	266 (23)	269 (18)	106 (11)	148 (18)	48 (13)	53 (11)
C(6)	533 (39)	196 (13)	113 (13)	−156 (19)	137 (18)	−9 (11)
C(11)	126 (9)	48 (3)	68 (6)	8 (4)	48 (6)	7 (3)
C(12)	168 (12)	55 (4)	134 (9)	20 (5)	91 (9)	15 (5)
C(13)	180 (13)	69 (5)	127 (9)	30 (6)	81 (9)	18 (5)
C(14)	110 (9)	94 (5)	84 (7)	−1 (6)	43 (7)	14 (5)
C(15)	183 (12)	57 (4)	108 (8)	−11 (6)	66 (8)	15 (4)
C(16)	155 (11)	49 (4)	110 (8)	3 (5)	74 (8)	5 (4)
C(21)	127 (9)	40 (3)	69 (6)	2 (4)	45 (6)	−5 (3)
C(22)	216 (14)	70 (5)	89 (7)	6 (6)	84 (9)	−15 (4)
C(23)	241 (16)	90 (6)	104 (8)	−11 (8)	74 (10)	−37 (6)
C(24)	207 (15)	63 (4)	101 (9)	−4 (6)	17 (9)	−35 (5)
C(25)	160 (13)	51 (4)	104 (8)	−12 (5)	35 (9)	−5 (4)
C(26)	153 (10)	40 (3)	80 (6)	4 (5)	46 (7)	−0 (3)
C(31)	133 (10)	50 (3)	83 (6)	7 (4)	52 (7)	12 (4)
C(32)	211 (14)	58 (4)	111 (8)	32 (6)	80 (9)	13 (4)
C(33)	270 (17)	59 (4)	184 (12)	55 (7)	145 (13)	20 (6)
C(34)	211 (15)	81 (5)	171 (11)	62 (7)	122 (11)	61 (6)
C(35)	262 (17)	99 (6)	111 (9)	64 (8)	83 (10)	49 (6)
C(36)	218 (15)	87 (5)	95 (7)	42 (7)	68 (9)	16 (5)

[a] In the form $\exp[-(\beta_{11}h^2 + \beta_{22}k^2 + \beta_{33}l^2 + 2\beta_{12}hk + 2\beta_{13}hl + 2\beta_{23}kl)]$.

$P(OMe)_3$ ligand with the sterically larger, more nucleophilic phosphine PMe_2Ph proceeds in a different manner to give as the major product complex **6** possessing two trans phosphines, a cis phosphite, and a single carbonyl group (Scheme IV). A subtle interplay of electronic and steric effects is probably responsible for the formation of this product, which is consistent with a rather strong Fe–$P(OMe)_3$ bond.

Finally, it is notable that displacement of η^2-CS_2 from **2** by other phosphorus ligands is not an important reaction path. This contrasts sharply with the usually facile displacement of olefins from (olefin) iron tetracarbonyls or other (olefin) metal carbonyl complexes by tertiary phosphines.

Crystal and Molecular Structure of $Fe(\eta^2\text{-}CS_2)(CO)_2(PMe_3)(PPh_3)$

The crystal structure consists of individual monomers separated by normal van der Waals contacts. An ORTEP plot of the structure of an individual molecule is shown in Figure 1. The iron atom is coordinated by the phosphorus atoms of two different phosphines in relative trans positions, two cis carbonyl groups, and the carbon and one sulfur atom of the CS_2 molecule. Stereochemically the molecule is best described in terms of a trigonal bipyramid with trans phosphines, two equatorial carbonyls, and the midpoint of the coordinated C=S bond of CS_2 occupying the third equatorial position. This description is supported by the P–Fe–P angle of 176.8 (0)°, the P(1)–Fe–CO (average 91.8°) and P(2)–Fe–CO (average 87.6°) angles, and planes 1–3 of Table IV. The principal structural feature of interest is the coordinated CS_2 ligand. A number of different bonding modes have been proposed for CS_2 including η^2 bonding analogous to that in olefin complexes, monodentate coordination via sulfur, and a four-electron bridging mode involving π electrons from a C=S bond and a lone pair on sulfur. Despite these predictions, X-ray analyses of CS_2 transition-metal complexes have so far been reported only for $Pt(CS_2)(PPh_3)_2$[14] and the analogous Pd complex,[15] confirming η^2-bonding modes. Convincing

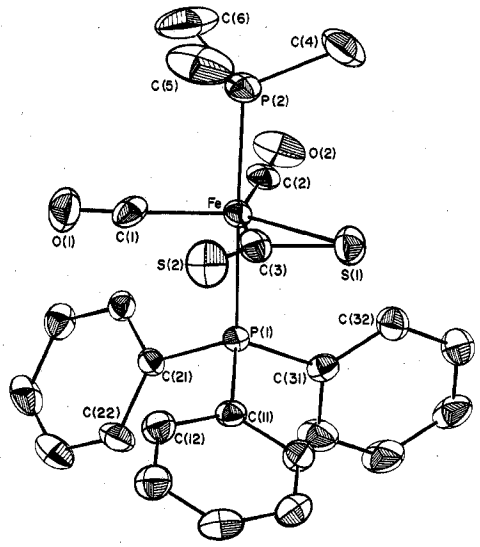

Figure 1. Perspective view of the molecular structure of $Fe(\eta^2\text{-}CS_2)(CO)_2(PMe_3)(PPh_3)$ showing the atomic numbering. Thermal ellipsoids represent 30% probability.

spectroscopic evidence has recently been produced for bridging of the CS_2 ligand in $(\eta^5\text{-}C_5H_5)(CO)_2MnCS_2Mn(CO)_2(\eta^5C_5H_5)$,[4] but no structural data are available. In the present case, the metal–CS_2 linkage resembles that in $Pt(CS_2)(PPh_3)_2$, but comparison of structural parameters for these two complexes is to a large extent precluded by the relatively high estimated standard deviations on bond lengths and angles in the platinum compound. Thus the C(3)–S(1) distance of 1.676 (7) Å in $Fe(\eta^2\text{-}CS_2)(CO)_2(PMe_3)(PPh_3)$ is not significantly different from the corresponding C–S distance of 1.72 (5) Å in $Pt(CS_2)(PPh_3)_2$ although both values differ from the C–S bond length of 1.554 Å in free CS_2. More significance can be attached to the observation that in $Fe(\eta^2\text{-}CS_2)(CO)_2$-

Table III. Bond Lengths (Å) and Angles (deg) for $Fe(\eta^2\text{-}CS_2)(CO)_2(PMe_3)(PPh_3)$

Distances

Fe-P(1)	2.279 (1)	C(12)-C(13)	1.369 (12)
Fe-P(2)	2.252 (2)	C(13)-C(14)	1.386 (11)
Fe-S(1)	2.334 (2)	C(14)-C(15)	1.371 (11)
Fe-C(1)	1.810 (6)	C(15)-C(16)	1.373 (12)
Fe-C(2)	1.771 (7)	C(16)-C(11)	1.388 (9)
Fe-C(3)	1.983 (8)	C(21)-C(22)	1.406 (9)
P(1)-C(11)	1.821 (7)	C(22)-C(23)	1.387 (11)
P(1)-C(21)	1.830 (5)	C(23)-C(24)	1.354 (13)
P(1)-C(31)	1.836 (6)	C(24)-C(25)	1.392 (10)
P(2)-C(4)	1.810 (11)	C(25)-C(26)	1.395 (9)
P(2)-C(5)	1.804 (12)	C(26)-C(21)	1.377 (9)
P(2)-C(6)	1.812 (16)	C(31)-C(32)	1.386 (9)
S(1)-C(3)	1.676 (7)	C(32)-C(33)	1.411 (11)
C(3)-S(2)	1.615 (8)	C(33)-C(34)	1.359 (12)
C(1)-O(1)	1.095 (8)	C(34)-C(35)	1.386 (12)
C(2)-O(2)	1.143 (10)	C(35)-C(36)	1.396 (13)
C(11)-C(12)	1.391 (9)	C(36)-C(31)	1.405 (9)

Angles

P(1)-Fe-P(2)	176.8 (0)	Fe-C(3)-S(1)	78.8 (0)
P(1)-Fe-S(1)	88.9 (0)	Fe-C(3)-S(2)	142.3 (0)
P(1)-Fe-C(1)	91.8 (2)	S(1)-C(3)-S(2)	138.9 (1)
P(1)-Fe-C(2)	91.8 (2)	Fe-C(1)-O(1)	178.0 (3)
P(1)-Fe-C(3)	93.7 (2)	Fe-C(2)-O(2)	177.0 (3)
P(2)-Fe-S(1)	91.4 (0)	P(1)-C(11)-C(12)	119.5 (3)
P(2)-Fe-C(1)	90.1 (2)	P(1)-C(11)-C(16)	122.4 (2)
P(2)-Fe-C(2)	85.1 (2)	C(16)-C(11)-C(12)	118.0 (4)
P(2)-Fe-C(3)	88.8 (2)	C(11)-C(12)-C(13)	120.9 (4)
S(1)-Fe-C(1)	136.9 (2)	C(12)-C(13)-C(14)	120.3 (4)
S(1)-Fe-C(2)	113.3 (2)	C(13)-C(14)-C(15)	119.1 (4)
S(1)-Fe-C(3)	44.8 (2)	C(14)-C(15)-C(16)	120.7 (4)
C(1)-Fe-C(2)	109.7 (3)	C(15)-C(16)-C(11)	120.8 (3)
C(1)-Fe-C(3)	92.3 (3)	P(1)-C(21)-C(22)	122.5 (3)
C(2)-Fe-C(3)	157.2 (2)	P(1)-C(21)-C(26)	119.8 (2)
Fe-P(1)-C(11)	115.1 (1)	C(26)-C(21)-C(22)	117.6 (4)
Fe-P(1)-C(21)	115.1 (1)	C(21)-C(22)-C(23)	120.1 (4)
Fe-P(1)-C(31)	115.7 (1)	C(22)-C(23)-C(24)	121.4 (4)
C(11)-P(1)-C(21)	103.4 (2)	C(23)-C(24)-C(25)	120.2 (4)
C(11)-P(1)-C(31)	104.7 (2)	C(24)-C(25)-C(26)	118.6 (4)
C(21)-P(1)-C(31)	101.2 (2)	C(25)-C(26)-C(21)	122.2 (3)
Fe-P(2)-C(4)	113.9 (3)	P(1)-C(31)-C(32)	122.1 (3)
Fe-P(2)-C(5)	117.3 (4)	P(1)-C(31)-C(36)	119.9 (3)
Fe-P(2)-C(6)	114.0 (4)	C(36)-C(31)-C(32)	118.0 (4)
C(4)-P(2)-C(5)	106.2 (5)	C(31)-C(32)-C(33)	120.3 (4)
C(4)-P(2)-C(6)	102.0 (5)	C(32)-C(33)-C(34)	121.3 (4)
C(5)-P(2)-C(6)	101.6 (6)	C(33)-C(34)-C(35)	119.1 (5)
Fe-S(1)-C(3)	56.4 (2)	C(34)-C(35)-C(36)	120.7 (5)
		C(35)-C(36)-C(31)	120.5 (4)

Table IV. Least-Squares Planes and Atomic Displacements Therefrom (Å) for $Fe(\eta^2\text{-}CS_2)(CO)_2(PMe_3)(PPh_3)$[a]

Plane 1: $-0.2554x - 0.0502y + 0.9655z + 5.3581 = 0$

Fe	−0.0464	C(2)	0.1037
S(1)	−0.0735	C(3)	0.0072
S(2)	0.0835	(O(1)	−0.0534)[b]
C(1)	−0.0745	(O(2)	0.2578)[b]

Plane 2: $-0.5910x + 0.8029y - 0.0781z + 4.0194 = 0$

Fe	−0.0376	P(2)	0.0187
P(1)	0.0184	midpt C(3)-S(1)	0.0006

Plane 3: $0.1256x + 0.9862y + 0.1082z + 3.4496 = 0$

Fe	−0.0123	P(2)	0.0064
P(1)	0.0063	C(2)	−0.0004

Plane 4: $0.9474x + 0.2076y + 0.2436z - 0.8823 = 0$

Fe	0.0339	P(2)	−0.0167
P(1)	−0.0165	C(1)	0.0007

[a] The dihedral angle between the planes Fe, C(1), C(2) and S(1), S(2), C(3) is 7.8°. [b] Not included in the derivation.

$(PMe_3)(PPh_3)$ *both* C(3)–S(1) (1.676 (7) Å) and C(3)–S(2) (1.615 (8) Å) bond lengths are longer than in the free ligand.[16] This suggests that coordination of CS_2 in η^2 fashion reduces the bond order of *both* C=S bonds. This result is relevant both to a ground-state description of the Fe–CS_2 interaction and to the reactivity and chemistry of the coordinated ligand. The common pictorial description of η^2-bound CS_2 is analogous to the Dewar–Chatt–Duncanson model for the metal–olefin bond. The extremes of I and II (Chart I) represent this description for η^2-CS_2. The net structural effect of forward σ donation from a CS_2 π MO to the iron and back-donation from iron to a π^* MO of CS_2 is a distortion of "free" CS_2 toward the geometry in the first excited state, with longer C–S bonds and an S–C–S angle <180°. In the $^3A_2$ excited state CS_2 has a bond length of 1.64 Å and an S–C–S angle of 135°.[17] These values compare favorably with a mean C–S bond length of 1.646 Å and an S–C–S angle of 138.9 (1)° in $Fe(\eta^2\text{-}CS_2)(CO)_2(PMe_3)(PPh_3)$. However, the individual C(3)–S(1) and C(3)–S(2) bond lengths indicate that neither of the two representations I and II nor a combination thereof provide an accurate or chemically useful description of the electron distribution in the coordinated CS_2 moiety. Two further models, III and IV, both of which imply dipolar character in the M–CS_2 fragment, must be considered. There are structural and chemical reasons for believing that III and IV contribute significantly. Thus the Fe–C(3) bond length (1.983 (8) Å) is markedly shorter than the Fe–C(acetylene) (average 2.063 Å) distances in the structurally related η^2-acetylene complex $Fe_2(CO)_6(Ph_2PC{\equiv}CPh)_2$,[18] the Fe–C(olefin) (average 2.151 Å) distances in $Fe(CO)_4(C_{12}H_8)$,[19] or the Fe–C(olefin) distances in a range of (diene)$Fe(CO)_3$[20] or (heterodiene)$Fe(CO)_3$[21] molecules. Indeed the Fe–C(3) distance more closely resembles the Fe–C(carbene) bond length of 1.945 Å in the iron(0)–carbene complex $Fe_2(CO)_6(PhCO)_2$.[22] Hence there is evidence for the metal–carbene bond character in the Fe–C(3) bond implied by III. Chemically, the uncoordinated sulfur atom in η^2-CS_2 complexes is undoubtedly nucleophilic, undergoing alkylation with a variety of electrophiles. The 1,3-dipolar character evident in III may also explain the facile cycloaddition of acetylenes to η^2-CS_2 complexes to yield five-membered metallocycles.[23] Clearly, in $Fe(\eta^2\text{-}CS_2)(CO)_2(PMe_3)(PPh_3)$ and η^2-CS_2 complexes some combination of the three forms II, III, and IV will best describe the electronic nature of the bound ligand with III and IV being particularly useful in predicting chemical reactivity.

Chart I

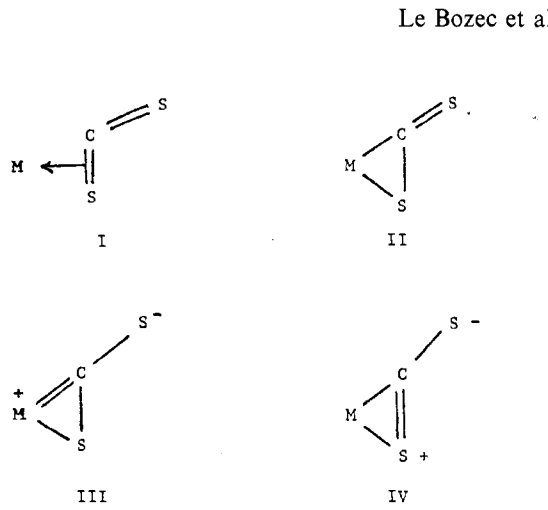

The iron–phosphorus distances (Fe–P(1) of 2.279 (2) Å and Fe–P(2) of 2.252 (2) Å) differ significantly from one another (Δ/σ = 13) with the shorter bond associated with trimethylphosphine. This difference may be rationalized on steric grounds (PMe_3 has a smaller cone angle than PPh_3)[13] or on the basis that with three acceptor ligands (2CO and CS_2) already present Fe(0) forms a stronger bond to the stroner σ donor, Me_3P of the two phosphines. The fact that the Fe–PMe_3 bond in $Fe(\eta^2\text{-}CS_2)(CO)_2(PMe_3)(PPh_3)$ is shorter and stronger than the Fe–PPh_3 bond is borne out by the transformation **3** → **5**. The PMe_3 ligands in compound **3** are

considerably more resistant to substitution than the PPh_3 ligands.

The Fe–P bond lengths in $Fe(\eta^2\text{-}CS_2)(CO)_2(PMe_3)(PPh_3)$ are both longer than those found in the trigonal-bipyramidal complexes *trans*-$Fe(CO)_3[P(OCH_2)_3P]_2$[24] (average 2.190 (4) Å) and $Fe(CO)_4(PPh_2H)$[25] (2.237 (2) Å). These differences may be attributable to the bidentate behavior of the CS_2 ligand and hence the presence of six atoms in the coordination sphere of iron. Similar Fe–P bond lengthening has been noted in the iron(0) acetylene complex $Fe_2(CO)_6(Ph_2PC{\equiv}CPh)_2$ where two acetylenic carbon atoms are coordinated to each iron.

Within the phosphines, bond distances and angles appear normal. The thermal motion of the methyl group carbon atoms in the trimethylphosphine ligand is evident from the thermal ellipsoids shown in Figure 1. There is an interesting comparison of Fe–P(1)–C(phenyl) (average 115.3°) and Fe–P(2)–C(methyl) (average 115.1°) angles for the two ligands. The similarity of these angles contrasts with the significant differences in corresponding angles in the complex $Fe(CO)_3[P(OCH_2)_3P]_2$.[24]

Spectroscopic Studies

Infrared Studies. All of the complexes **2a–g**, **3**, **4**, **5**, and **6** exhibit an absorption band in the infrared between 1135 and 1170 cm^{-1} corresponding to the uncoordinated ν(C=S) vibration. These frequencies are much lower than the value of 1523 cm^{-1} for ν_2 in free CS_2, consistent with a significantly longer C=S (uncoordinated) bond length in the complex than in free CS_2. There appears to be some correlation of ν(C=S) frequencies with the electron-acceptor properties of the phosphorus ligand. Thus **2a**, **2b**, and **2c** with $P(OR)_3$ ligands have higher ν(C=S) values than **2e**, **2f**, and **2g** with phosphines. Unfortunately, in the ν(C=S) region of the spectrum, coupling with other ligand modes may be severe and it is doubtful whether much significance can be attached to the absolute values of these frequencies either here or in other CS_2 containing molecules.[2b]

Compounds **2a–g**, **3**, **4**, and **5** show two bands arising from carbonyl vibrations. The corresponding ν(CO) frequencies are strongly influenced by the presence of ligands L. As generally observed, their magnitude is higher for phosphites, the poorer donor in **2a**, **2b**, and **2c**, than for phosphines. The frequencies (or calculated force constants k_{CO}[26] when available) of complexes $Fe(\eta^2\text{-}CS_2)(CO)_2L_2$ can be compared with those of the corresponding derivatives $Fe(CO)_3L_2$. Thus comparison of the pairs **2a** (2020, 1964 cm^{-1} (THF), k_{CO} = 16.04 mdyn $Å^{-1}$) and $Fe(CO)_3[P(OMe)_3]_2$ (2002, 1916 cm^{-1} (hexane), k_{CO} = 15.29 mdyn $Å^{-1}$),[27] **2d** (1999, 1937 cm^{-1} (CH_2Cl_2),[28] k_{CO} = 15.66 mdyn $Å^{-1}$) and $Fe(CO)_3(PPh_3)_2$ (1973, 1886 cm^{-1} (CH_2Cl_2), k_{CO} = 14.83 mdyn $Å^{-1}$), **2f** (1999, 1933 cm^{-1} (THF)) and $Fe(CO)_3(PMe_2Ph)_2$ (1883 cm^{-1} (C_6H_{14})),[29] and **5** (2010, 1943 cm^{-1} (THF)) and $[P(OCH_2)_3P]Fe(CO)_3[P(OCH_2)_3P]$ (1927 cm^{-1} (CH_2Cl_2))[24] shows that the η^2-CS_2 ligand bonded to Fe(0) behaves as a much stronger electron-withdrawing group than coordinated carbon monoxide. Similar behavior has also been observed for the η^2-CS_2 ligand bonded to manganese.[6]

NMR Studies. ^1H NMR spectra exhibit virtual coupling for the symmetrical complexes $Fe(\eta^2\text{-}CS_2)(CO)_2L_2$ **2a**, **2e**, **2f**, and compound **6**. Such coupling indicates the virtual trans positions of identical phosphorus ligands L. Moreover, when L is PMe_2Ph, the methyl groups appear to be nonequivalent. The diastereotopy appears very clearly in **6** which contains three different ligands in the equatorial plane. In contrast, the difference in chemical shift is small in compound **2f** when the diastereotopy is created only by the dissymmetry of the η^2-CS_2 ligand.

The coupling of methyl protons with the trans ^{31}P nuclei could be observed only in the case of compounds containing trimethylphosphine: $^4J_{P-H}$ = 1.1 Hz (**3**) or 2.0 Hz (**5**).

The ^{31}P FT NMR spectra are unambiguously consistent with the proposed structure for symmetrically substituted complexes **2d**, **2f**, **2e**, and **2g** for which only one line is observed and for the unsymmetrically substituted derivatives **3** and **5** which show clear AB- or AX-type patterns.

Compound **6** shows equivalent *trans*-dimethylphenylphosphines and allows the measurement of a cis coupling constant: $^2J_{P-P}$ = 55.7 Hz for a η^2-CS_2–Fe complex.

Trans $^2J_{P-P}$ values are relatively high. The value of $^2J_{P-P}$ which is 161 Hz in $Fe(CS_2)(CO)_2(PMe_3)(PPh_3)$ increased to 245 Hz in **5** when triphenylphosphine was replaced by trimethyl phosphite. This increase of the ^2J value is related in part to the increased electronegativity of the substituents bonded to phosphorus. A higher electronegativity for a substituent on phosphorus concentrates the "s" character in the phosphorus lone-pair orbital, and this is reflected in a larger coupling constant between phosphorus nuclei sharing the same metal orbitals. Similar trends have been noted for $M(CO)_4(PR_3)_2$ derivatives (M = Cr, Mo, W).[30] However, since our synthetic results clearly indicate that the Fe–$P(OMe)_3$ bond is more robust than the Fe–PPh_3 bond, it is possible that electronic or steric effects related to the stability of the Fe–P bond other than a change in phosphorus lone-pair "s" character also contribute to the high value of $^2J_{P-P}$. The magnitude of the ^2J value for compound **5** can be compared with that of the analogously disubstituted iron(0) complex $P(OCH_2)_3P$-$Fe(CO)_3P(OCH_2)_3P$[24] ($^2J_{P-P}$ = 38 Hz). This indicates that we might expect an increase of the J value when one CO is replaced by a η^2-CS_2 ligand, although in the latter compound the lengths of the iron–phosphorus bonds are expected to be shorter than in **5** because of the small cone angle for bicyclic phosphorus ligands and the larger number of atoms in the coordination sphere of iron in the η^2-CS_2 complex.

Acknowledgment. This work was supported in part by operating grants from the National Research Council of Canada (A.J.C.). H.L.B. is grateful to the DGRST for the award of a studentship.

Registry No. **1**, 38333-35-6; **2a**, 64424-66-4; **2b**, 64424-67-5; **2c**, 66808-76-2; **2d**, 64424-68-6; **2e**, 64424-58-4; **2f**, 64424-57-3; **2g**, 64424-69-7; **3**, 64424-59-5; **4**, 64424-60-8; **5**, 66808-75-1; **6**, 66808-74-0.

Supplementary Material Available: A listing of structure factor amplitudes, hydrogen atom coordinates and isotropic thermal parameters (Table S1), and carbon–hydrogen bond lengths (Table S2) (13 pages). Ordering information is given on any current masthead page.

References and Notes

(1) (a) Université de Rennes. (b) University of Waterloo.
(2) (a) I. S. Butler and A. E. Fenster, *J. Organomet. Chem.*, **66**, 161 (1974); (b) T. J. Collins, W. R. Roper, and K. G. Town, *J. Organomet. Chem.*, **121**, C41 (1976).
(3) K. R. Grundy, R. O. Harris, and W. R. Roper, *J. Organomet. Chem.*, **90**, C34 (1975).
(4) M. Herberhold, M. Suss-Fink, and C. G. Kreiter, *Angew. Chem., Int. Ed. Engl.*, **16**, 193 (1977).
(5) I. S. Butler, N. J. Coville, and D. Cozak, *J. Organomet. Chem.*, **133**, 59 (1977). Insertion of CS_2 into the iron–iron bond of $(\eta^5\text{-}C_5H_5)_2Fe_2(CO)_4$ yielding $(\eta^5\text{-}C_5H_5)(CO)_2FeCS_2Fe(CO)_2(\eta^5\text{-}C_5H_5)$ has also been reported (J. E. Ellis, F. W. Fennell, and E. A. Flom, *Inorg. Chem.*, **15**, 2031 (1976)) but this molecule is formulated as a metallodithiocarboxylate.
(6) M. Herberhold and M. Suss-Fink, *Angew. Chem., Int. Ed. Engl.*, **16**, 194 (1977).
(7) J. A. S. Howell, B. F. G. Johnson, P. L. Josty, and J. Lewis, *J. Organomet. Chem.*, **39**, 329 (1972).
(8) M. C. Baird, G. Hartwell, and G. Wilkinson, *J. Chem. Soc. A*, 2037 (1967).
(9) A referee has pointed out that according to crystallographic convention, the reduced cell in space group *Pn* with a = 9.309, b = 13.640, and c = 10.440 Å and having a less obtuse β angle of 109.82° ought to have been used. Although crystallographically unconventional, our choice of the *Pc* cell does not in any way invalidate the structure analysis, derived molecular parameters, or structural conclusions drawn from the X-ray study.

(10) "International Tables for X-ray Crystallography", Vol. III, Kynoch Press, Birmingham, England, 1962, pp 202–211.
(11) R. F. Stewart, E. R. Davidson, and W. T. Simpson, *J. Chem. Phys.*, **42**, 3175 (1965).
(12) A. Vessieres, D. Touchard, and P. Dixneuf, *J. Organomet. Chem.*, **118**, 93 (1976).
(13) C. A. Tolman, *J. Am. Chem. Soc.*, **92**, 2956 (1970).
(14) R. Mason and A. I. M. Rae, *J. Chem. Soc. A*, 1767 (1970).
(15) T. Kashiwagi, N. Yasuoka, T. Ueki, N. Kasai, and M. Kakudo, *Bull. Chem. Soc. Jpn.*, **40**, 1998 (1967).
(16) A. H. Guenther, *J. Chem. Phys.*, **31**, 1095 (1959).
(17) B. Kleman, *Can. J. Phys.*, **41**, 2034 (1963).
(18) A. J. Carty, H. N. Paik, and G. J. Palenik, *Inorg. Chem.*, **16**, 300 (1977).
(19) F. A. Cotton and P. Lahuerta, *Inorg. Chem.*, **14**, 116 (1975).
(20) A. J. Carty, N. J. Taylor, and C. R. Jablonski, *Inorg. Chem.*, **15**, 1169 (1976).
(21) A. De Cian and R. Weiss, *Acta Crystallogr., Sect. B*, **28**, 3264 (1972).
(22) P. F. Lindley and O. S. Mills, *J. Chem. Soc. A*, 1279 (1969).
(23) Y. Wakatsuki, H. Yamazaki, and H. I. Wasaki, *J. Am. Chem. Soc.*, **95**, 5781 (1973).
(24) D. A. Allison, J. Clardy, and J. G. Verkade, *Inorg. Chem.*, **11**, 2804 (1972).
(25) B. T. Kilbourn, U. A. Raeburn, and D. J. Thompson, *J. Chem. Soc. A*, 1906 (1969).
(26) Force constants were calculated by the method of F. A. Cotton and C. S. Kraihanzel, *J. Am. Chem. Soc.*, **84**, 4432 (1962). Other values (mdyn Å^{-1}) not mentioned in the text are as follows: **2b**, 15.99; **2c**, 16.22; **2f**, 15.62; **2g**, 15.52; **3**, 15.58; **4**, 15.66; **5**, 15.79; **6**, 14.65.
(27) A. Reckziegel and M. Bigorgne, *J. Organomet. Chem.*, **3**, 341 (1965).
(28) T. A. Manuel and F. G. A. Stone, *J. Am. Chem. Soc.*, **82**, 366 (1960).
(29) H. L. Conder and M. Y. Darensbourg, *J. Organomet. Chem.*, **67**, 93 (1974).
(30) F. B. Ogilvie, J. M. Jenkins, and J. G. Verkade, *J. Am. Chem. Soc.*, **92**, 1916 (1970).

Contribution from Union Carbide Corporation, Chemicals and Plastics Division, South Charleston, West Virginia 25303

$[Rh_{17}(S)_2(CO)_{32}]^{3-}$. 1. An Example of Encapsulation of Chalcogen Atoms by Transition-Metal–Carbonyl Clusters

JOSÉ L. VIDAL,* R. A. FIATO, L. A. COSBY, and R. L. PRUETT

Received December 14, 1977

The reaction of a solution of $Rh(CO)_2acac$ and alkali carboxylates in a glyme solvent, with H_2S or SO_2 under ~300 atm of carbon monoxide and hydrogen at 140–160 °C, resulted in the isolation of $[C_6H_5CH_2N(C_2H_5)_3]_3[Rh_{17}(S)_2(CO)_{32}]$. The complex has been characterized via a complete three-dimensional X-ray diffraction study. The complex crystallizes in the primitive monoclinic space group $P2_1/n$, with a = 14.990 (2) Å, b = 38.458 (10) Å, c = 16.206 (3) Å, β = 101.26 (3)°, V = 9163 (1) Å^3, and ρ (calcd) = 2.383 g cm^{-3} for mol wt 3286.83 and Z = 4. Diffraction data were collected with an Enraf-Nonius CAD 4 automated diffractometer using graphite-monochromatized Mo Kα radiation. The structure was solved by direct methods and refined by difference-Fourier and least-squares techniques. All nonhydrogen atoms have been located and refined; final discrepancy indices are R_F = 5.0% and R_{wF} = 6.6% for all 12 820 symmetry-independent reflections in the range $0° \leq 2\theta \leq 45°$. The structure consists of 16 rhodium atoms distributed in the corners of four stacked, parallel squares and of a S–Rh–S group located inside the cluster. Rhodium–rhodium bonding and nonbonding distances of 2.76–2.88 and ~3.40–3.60 Å, respectively, are found in the structure. The sulfur–rhodium lengths, 2.17 and 2.33 Å, are shorter than the sum of the covalent radii of the two elements. Average values for the terminal and bridging rhodium–carbon and carbon–oxygen lengths are in the ranges of 1.81–1.85 and 1.98–2.03 Å and 1.14–1.18 and 1.18–1.20 Å, respectively. The unusual chemical stability of $[Rh_{17}(S)_2(CO)_{32}]^{3-}$ is shown by its inertness to strongly basic or acidic conditions. The anion exhibits Brønsted acid–base chemistry consistent with

$$[Rh_{17}(S)_2(CO)_{32}]^{3-} \underset{2OH^-}{\overset{2H^+}{\rightleftharpoons}} \text{"}[Rh_{17}(S)_2(CO)_{32}H_2]^-\text{"}$$

as indicated by infrared and elemental analysis. ^{13}C solution NMR results are consistent with the solid-state structure indicating that it is maintained in solution. Some evidence is also presented which suggests that the anion is able to activate hydrogen at ambient conditions.

Introduction

Transition-metal–carbonyl clusters have attracted growing attention in the literature.[1-4] Much of this interest has been generated by the involvement of these compounds in a variety of catalytic reactions[3-16] and by the novel chemical behavior which they have exhibited.[3-19] Extra incentive for structural studies was provided by the opportunity offered for testing bonding theories.[1-3]

There are a number of examples of polynuclear metal clusters which contain isolated main-element atoms coordinated to the metal polyhedra. Isolated carbon atoms of the carbide type have been reported for systems in which this atom either is incompletely surrounded by metal atoms, as in $Fe_5(CO)_{15}C$,[20] or is completely coordinated to these atoms and placed inside the cavity of the metal polyhedra, as in $[Rh_6(CO)_{15}C]^{2-}$.[21] Further examples of transition-metal–carbonyl clusters containing coordinated main-element atoms in a fashion resembling that of $Fe_5(CO)_{15}C$ are provided for silicon ($[Co_4Si(CO)_{13}]$[22]), for phosphorus ($[Co_4(\eta^5\text{-}C_5H_5)_4P_4]$[23]), for arsenic ($[As_2(CO)_2(CO)_6]$[24]), and for sulfur, selenium, and tellurium ($[X_2Fe_3(CO)_9]$ (X = S, Se, Te)[25]).

Atomic sulfur is reported[26] to be a versatile ligand toward transition-metal complexes and the following modes of linkage are described: (1) a double-bridging, two-electron-donating ligand in $[Mo_2(\eta^5\text{-}C_5H_5)_2(O)_2(\mu\text{-}S)_2]$ and in $[Mo_3(\eta^5\text{-}C_5H_5)_3S_4]$; (2) a triply bridging, four-electron-donating, trigonal-pyramidal-like ligand in $[Co_3(CO)_9S]$, $[Co_3(\eta^5\text{-}C_5H_5)_3S_2]$, and $[Co_4(\eta^5\text{-}C_5H_5)_4S_4]$; (3) a quadruply bridging, four-electron-donating, square-pyramidal-like ligand in $[Co_4(CO)_{10}(S)_2]$; and (4) a quadruply bridging, six-electron-donating, tetrahedral-like ligand in $[Fe_2(CO)_6(\mu\text{-}SCH_3)]_2S$- and in $[Re_2Mo(\eta^5\text{-}C_5H_5)(CO)_8]S[SMo(\eta^5\text{-}C_5H_5)(CO)_3]$. An in-depth study of these compounds has been done by Dahl's group.[23-33]

Other high-nuclearity transition-metal–carbonyl clusters have been found to encapsulate metal atoms, e.g., $[Rh_{13}(CO)_{24}H_{5-n}]^{n-}$,[12,34] and isolated carbon atoms, e.g., $[Rh_8(CO)_{19}C]$,[35] $[Rh_{12}(CO)_{25}(C)_2]$,[36] and $[Rh_{15}(CO)_{28}(C)_2]^-$.[37] In

0020-1669/78/1317-2574$01.00/0